Origins of solidification when a simple molecular fluid is confined between two plates

A. Levent Demirel
Chemistry Department, Koç University, Rumelifeneri Yolu, Sariyer 80910, Istanbul, Turkey

Steve Granick
Department of Materials Science and Engineering, University of Illinois, Urbana, Illinois 61801

(Received 5 January 2001; accepted 27 April 2001)

A simple globular-shaped liquid (octamethylcyclotetrasiloxane, OMCTS) was placed between two rigid mica plates at variable spacings comparable to the size of this molecule and the linear shear viscoelasticity of the confined interfacial film was measured. Strong monotonic increase of the shear relaxation time, elastic modulus, and effective viscosity were observed as the spacing was decreased below about 10 molecular dimensions. The frequency dependence of the viscoelastic spectra measured at different film thicknesses appeared to scale with reduced variables. The data are inconsistent with the abrupt first-order transition, from bulk fluid to solid with decreasing film thickness, whose possibility has been hypothesized, and suggest a glasslike transition instead. © *2001 American Institute of Physics.* [DOI: 10.1063/1.1380207]

I. INTRODUCTION

Mechanical shear experiments performed since the late 1980s show that simple low-viscosity fluids ''solidify'' when confined to molecularly-thin spacings between opposed single crystals of mica[1,2] or between mica coated with self-assembled organic monolayers that lack long-range crystalline order.[3] Since the discovery of this phenomenon, much has been written seeking to interpret the molecular origin of ''solidification,'' of which the laboratory signature is that sliding motion over a macroscopic distance cannot be accomplished unless a yield stress is exceeded. There has been controversy between those claiming that the effect originates in a first-order transition from liquidlike to solidlike behavior, and others who lean towards a continuous transition to a glassy state.

Solidification in these systems contrasts with confinement of fluids within small pores, where confinement causes shifts of the melting, freezing, and vitrification transitions towards *lower* temperatures.[4,5] Eventually, for films a few molecular diameters thick, these transitions become smeared and almost vanish entirely.[6] One difference is probably that confinement under constant load can readjust the film thickness slightly to optimize molecular packing; there may also occur small shifts of the confining solid surfaces to achieve this effect. A second difference may be related to the ''surface-T_g'' problem of thin films against air, which recently has become an active field of study.[7] Concerning that problem it is increasingly clear that different research probes (which may be as diverse as calorimetry, dielectric response, thermal expansion coefficient, transport properties, and computer simulations[1,2,4–7]) generate findings that are in some cases difficult to reconcile—a fact that has rendered this field of study rather controversial. A third difference concerns the molecular interpretation of ''solidity.'' This paper will argue that it is a ''soft'' solidity and not to be identified with a phase transition.

The problem is how to interpret the shear rheology of molecularly-thin films in a surface forces apparatus. Solidity in force-based experiments using the surface forces apparatus was at first unequivocably identified with crystallinity[1,2]—it was at first presumed that solidification must represent a transition to some kind of periodic molecular array with long-range order. Yet the amorphous solid state is surely another possibility in principle whenever a sample displays mechanical stiffness.[8] Several reviews, written from opposing points of view, summarize current uncertainties concerning confined fluid films.[9–12] It continues to be argued that the very observation of yield stress signifies that solidification represents crystallization induced by confinement.[11–14] If so, solidification is a phase transition and kinetic sliding represents shear-induced melting. Given the fact that crystallization is a first-order phase transition, it was desirable to test, by direct experiment, whether the transition is first-order or not, and this was the first goal of the experiments reported below.

This laboratory has argued that the transition from fluidity to solidity is ''glass like'' with diminishing film thickness, the force squeezing two surfaces together playing a role analogous to the more familiar variables of temperature or pressure.[7,9,10,15] If so, shear stiffness reflects some kind of disordered state whose transition to solidity may be continuous. Similarly, kinetic sliding is then analogous to flow in a granular material[16] and to shear-induced unjamming.[17] The experiments presented below present new evidence in favor of this interpretation.

The many computer simulations that address this problem have supported both points of view, depending on the simulation model. Crystalline structure is seen in molecularly-thin films of fluid particles whose size is nearly the same as atoms in the confining solid. The particle then fits into potential wells of the corrugated surface and epitaxial alignment with the solid surface is possible.[18–20] This breaks down unless the solid surfaces are aligned to be in

 © 2001 American Institute of Physics

Downloaded 25 Jul 2001 to 130.126.103.150. Redistribution subject to AIP license or copyright, see http://ojps.aip.org/jcpo/jcpcr.jsp

registry with one another. If the fluid particle is larger, or if the solid surfaces are misaligned, then structures may form that are incommensurate with the solids[20,21] and, alternatively, amorphous packing may result.[22] Predictions of confined fluid structure evidently depend on details of the simulation model. To the authors of this paper, it seems unlikely that the ubiquitous observation of solidity in laboratory experiments can be explained as an effect of having crystalline solid surfaces that are in strict registry.

The issue of solidity may also be addressed by measuring kinetic properties such center-of-mass diffusion in the rest state. A limited set of molecular dynamics (MD) computer simulations have been performed with this purpose in mind. Attention has focused on diffusion parallel to the confining walls (the rate of diffusion perpendicular to walls of molecularly-thin spacing not being well-defined in the usual sense). These studies show that the center-of-mass diffusion coefficient slows down with decreasing film thickness, appearing to oscillate with film thickness as do force measurements.[20] The amount of slowing down relative to bulk diffusion rates has been reported to be a factor of 30–100.[20,22] Unfortunately these studies report diffusion averaged over the film. As Schweizer has noted,[23] molecules closer to the walls should be most ordered (least mobile) and molecules closest to the center of the film should be least ordered (most mobile). It would be arguably more relevant, when considering the transfer of stress from one solid surface to another, to consider molecules at the center of the confined film.[23] Regardless, it appears that the arrest of translational mobility on the MD time scale, as would be expected of crystalline order, has not been observed to date.

Many computer simulations on confined fluid systems involve sliding. Computations about dynamics are so time-consuming, however, that in order to exceed the rate of thermal motion, the lowest rate of externally-driven flow that can be studied is presently $\approx 10^7\ \mathrm{s}^{-1}$ (and, in many of the reported simulations, still higher than this). These very high rates leave unclear whether, at lesser rate, the confined liquid would be solid or fluid. To resolve this issue, a measurement should involve linear-response in order to rule out the possibility of shear-induced changes. A recent molecular dynamics simulation in which pains were taken to achieve linear response did observe a smooth transition, with diminishing thickness, towards slower relaxation.[24]

To put this problem in context, the fundamental interest in liquids confined between two parallel solid surfaces started increasing during the 1970s with the availability of the surface forces apparatus (SFA) technique. It is true that many other measurements have also concerned fluids confined within porous solid media, which have the advantage of a vastly larger surface area and therefore larger sample volume, but this confining geometry suffers from nonuniformity. Furthermore, it is not feasible to vary either the pore size continuously, and not feasible to apply external shear fields that are well-defined. The SFA technique, in contrast, made possible direct measurements of the interaction of two surfaces as a function of surface separation with an intervening liquid between the two.[25] The experiments are performed when this fluid is confined between mica, a crystal that can readily be cleaved to produce atomically smooth and step-free areas of $\approx \mathrm{cm}^2$. The advantage is that surface separations of intervening films are defined with a resolution of angstroms. Many of the early experimental studies on confined liquids concentrated on static measurements, i.e., the interaction of the surfaces through the liquid film as a function of film thickness, which is usually referred as force-distance profile.

The first force-distance profile of a hydrocarbon liquid confined between atomically smooth mica surfaces was reported for OMCTS, $[(CH_3)_2SiO]_4$, octamethylcyclotetrasiloxane, considered to be a model liquid for comparison with the theoretical concept of a ''Lennard-Jones'' liquid because of the globular shape of this ring-shaped nonpolar molecule.[26–28] OMCTS is a compact, cyclic-shaped molecular liquid with eight pendant methyl groups. It is approximately globular with a diameter of ~ 9 Å.[26] The melting temperature of 18 °C is close to the temperature of most experiments in this field (room temperature), which sparked the suggestion, from early days, that the melting point of OMCTS might be elevated by confinement.[27] However, force-distance relations of OMCTS display minimal dependence on temperature when this is varied from room temperature to below the bulk melting temperature.[27]

Below a surface separation of ~ 70 Å, the force-distance profile of OMCTS shows spatial oscillations with periodicity equal to the size of the molecules and the amplitude decaying exponentially with increasing surface separation. At very small surface separations the local ordering induced by the two separate boundaries begins to overlap and to interfere constructively, or destructively, thus generating oscillatory forces. The maximal forces occur when the surface separation is close to an integer number of molecular diameters. Then the molecules can pack efficiently in distinct layers and the density is high within the molecular layers. The minimal forces occur when the surface separation is around an integer and a half multiple of the molecular diameter. In these cases, it is not possible to utilize the space very efficiently so the density is low and the structure is more diffuse. (However for alkane molecules of more complex shape, computer simulations show that the force-distance relations and density profiles do not have a one-to-one relationship.[29])

Comparison of such experiments to theory and computer simulation rests on the Derjaguin approximation, $F(D)/R = 2\pi W(D)$. Here $F(D)$ is the force needed to bring two curved surfaces of mean radius of curvature R ($R \approx 2$ cm is typical in SFA experiments) to a closest spacing D; and $W(D)$ is the energy per unit area of two parallel surfaces separated by spacing D. In laboratory experiments, $F/R \approx 1-10\ \mathrm{mN\,m}^{-1}$ is typical, which amounts to 0.15–1.5 $\mathrm{mJ\,m}^{-2}$. This in turn is equivalent to $0.04-0.4\ k_BT$ per nm^2. Here we consider the cross-sectional area of 1 nm^2 because it is roughly the cross section of the globular-shaped OMCTS molecule that has been considered to be the prototypical simple molecular fluid in this field of study.

This weak layering explains why it is possible to pass sequentially to smaller-and-smaller film thickness simply by applying increasing compressive force to a confined liquid—a transition that would not be feasible to effect in the

Downloaded 25 Jul 2001 to 130.126.103.150. Redistribution subject to AIP license or copyright, see http://ojps.aip.org/jcpo/jcpcr.jsp

case of an ordinary macroscopic crystal. The tendency of the liquid to organize in strata parallel to a solid body is very weak on a per molecule basis. It is observed only because of the very high force sensitivity of the SFA [stratification of OMCTS has, more recently, also been observed using atomic force microscopy (AFM) (Ref. 30)].

Oscillatory force-distance profiles are also observed with linear alkanes, C_nH_{n+2}, which are flexible chain molecules.[28] The period of the oscillations is close to the expected molecular thickness of 4 Å; this indicates that the molecular axes are preferentially oriented parallel to the surfaces. Flexibility of linear molecules hinders efficient packing, so the magnitude and range of these oscillations are less than those of globular molecules. The magnitude and range of the oscillations in the normal force decrease further as the shapes of the molecules become more irregular by addition of CH_3 side groups to linear chain molecules as branches. Adding one side group does not prevent the oscillations completely; 3-methylundecane, $CH_3(CH_2)_7CH(CH_3)CH_2CH_3$, displays oscillatory forces.[3] For squalane, $(CH_3[CH(CH_3)(CH_2)_3]_2CH(CH_3)CH_2CH_2)_2$, with 6 CH_3 side groups attached to the backbone, the force-distance profile is not oscillatory but has only a single attractive minimum at a thickness of 18 Å^3, although computer simulations predict that the density profile nonetheless is layered.[29]

A common observation in many (but not all) shear experiments and shear simulations is the observation of ''stick-slip:'' the fluid film responds elastically when the applied force is small but appears to break up when a critical level, the ''yield stress,'' is exceeded. Indeed, when a system, whether in the bulk or confined, is sheared at small enough strain amplitudes that the equilibrium structure is weakly perturbed, but at a rate faster than the reciprocal of the longest relaxation time, the system cannot respond so fast and appears to be frozen.[31] It is important to appreciate that this is not a change in the physical state of the system, but just a change in the response of the system because of the limited time given to respond.

We turn now to the issue of shear stiffness and shear viscosity. In the case of shearing liquids, for a given terminal relaxation time, τ_1, when the shear rate, γ', is smaller than $1/\tau_1$, the dissipative properties dominate, as the liquid has enough time to relax the stress imposed by the external shear by conformational changes and thus dissipate energy. When $\gamma' > 1/\tau_1$, the liquid can not relax as much in the given time. Less energy is dissipated and the elastic properties dominate. Experiments of this kind[3,10,15,32,33] show that the dynamic variables such as the viscosity and relaxation times are affected significantly by confinement. With decreasing surface separation, the longest relaxation time of molecularly-thin films was prolonged and the viscosity enhanced by orders of magnitude over that of the bulk. The entire film shows a gradual switch, over a range of a few molecular diameters of film thickness, from predominantly viscous to predominantly elastic response. Pains were taken to perform these phenomena in the limit of linear viscoelastic response so that it would be certain that the act of measurement did not perturb the system being measured.

Recent experiments involving the shear of OMCTS (Refs. 13, 14) and other confined small-molecule fluids[14] were interpreted to show a first order dynamic phase transition to a solid structure. However, the shear rates in those experiments were so large that the responses should have been highly nonlinear. For comparison, it is worthwhile to check the linear responses. We recently studied in detail the transition from linear- to nonlinear-response in the OMCTS system.[34] Of special significance was the demonstration that stick-to-slip transitions were observed routinely when films were subjected at stimulating frequencies faster than the terminal relaxation time.

A brief account of the experiments described below has appeared previously.[15] The aims of the paper that follows were as follows:

(1) Given that crystallization is a first-order phase transition, we have sought to determine, by direct experiment, whether confinement-induced solidification is first-order or not;
(2) Given that the act of shear may induce structural changes, we have sought, in order to rule out this possibility, to perform all these measurements in the limit of linear response;
(3) Given that a liquid's viscoelastic stiffness can limit its capacity to respond to rapid deformation (rather like the viscoelasticity of that childrens' plaything, Silly Putty), we have sought to perform these measurements over a wide spectrum of deformation rate, spanning several logarithmic decades.

II. EXPERIMENT

Recently, new shear attachments were developed in this laboratory for use with the SFA technique.[1,2,32,33,35,36] These attachments allow the two surfaces to be sheared past each other at varying sliding speeds in steady shear or oscillatory shear, while simultaneously measuring both the shear and the normal forces. Oscillatory shear attachment was employed in the experiments presented here.

Oscillatory shear modification to SFA is accomplished by mounting the top surface to a small boat rigidly attached to two piezoelectric bimorph strips, for which the dominant motion is bending. The other ends of the bimorphs are fixed in a base support by an epoxy glue. To increase flexibility, each bimorph is lengthened at one end with a short strip of more flexible steel spring by gluing the two. Shear is induced when a voltage difference applied between the two sides of one of the bimorphs bends it. The resulting displacement is transferred to the other bimorph through the rigidly attached boat inducing a voltage difference between the two sides. The comparison of this output voltage when the surfaces are apart, called the calibration output, with that when the surfaces are in contact with an intervening fluid gives information about the response of the fluid to the applied shear. The viscoelasticity of the fluid confined between the two surfaces resists the applied shear motion and results in amplitude attenuation and phase shift with respect to the output voltage when the surfaces are apart.

The surfaces, atomically smooth sheets of muscovite mica, are silvered on one side for interferometry and the

Downloaded 25 Jul 2001 to 130.126.103.150. Redistribution subject to AIP license or copyright, see http://ojps.aip.org/jcpo/jcpcr.jsp

silvered side is mounted with an adhesive onto silica disks with cylindrical shape. The top and bottom surfaces are oriented in a cross cylinder configuration. When the two surfaces are brought together in this configuration, they touch each other at one point. Due to the compliance of the underlying adhesive the surfaces flatten under the action of adhesive forces and the normal load, producing a region of contact in which the surfaces are locally planar and parallel. In the case of a simple nonpolar liquid between the surfaces, this flattening happens at very small surface separations (<50 Å) when the fluid forms a structure that can support the normal load. The onset of flattening approximately corresponds to the surface separation where the differences in the amplitude and phase of the output voltage with respect to the calibration output start.

The mechanical and the electrical characteristics of the shear device, together with the mechanical behavior of the intervening liquid, was previously modeled and expressions relating the measured amplitude attenuation and the phase shift to the apparent dynamic viscosity and the elastic modulus of the liquid were derived.[35,36] The mechanical model replaces the device, glue and the liquid with a combination of effective masses, springs and dashpots. Simply put, a complex impedance, $Z_D = k_D + i\omega b_D$, can be assigned to the device, which responds like an underdamped forced harmonic oscillator when a voltage is applied to the input terminals.

Here the real part of the impedance represents the equivalent spring constant of the device, a combination of the spring constants of the bimorphs and the leaf springs. The imaginary part is due to the dissipation in the system, mostly caused by the adhesive that holds the bimorphs to the leaf springs. In this configuration the applied stress is split into two, between the device and the combination of glue and liquid. The resulting displacement is the sum of the displacement of the glue and the displacement of the liquid. However, with changing liquid impedance, neither the force nor the displacement of the liquid is constant in time due to this parallel configuration, unlike the traditional viscoelastic measurements where either the stress or the strain is kept constant and the change of the other parameter is observed in time. This has the advantage of observing the transient time effects, namely, how the force and the displacement of the liquid evolve to their steady state values when a change in the state of the liquid happens.

In practice, even below the main resonance frequency of the device, some frequency regions must be avoided when the top and bottom surfaces are in contact and coupling strongly. When two mica surfaces are in contact the main resonance peak is moved to slightly lower frequencies because of the increased equivalent mass of the system. In addition, several other resonance peaks are also observed. The amplitude of these resonance peaks depends on the stiffness of the interface. Even in the case of an intervening liquid between the surfaces these resonance peaks were observed and their amplitudes increased as the response of the liquid became predominantly elastic with decreasing film thickness. Such resonance peaks could in principle be used to get information about the stiffness of the intervening liquid. For the shear measurements described below, such resonance peaks were avoided by choosing the oscillation frequencies accordingly in order to be able to apply the abovementioned mechanical model for the analysis of the data.

In the output circuit, the finite input resistance of the measuring device is in parallel with the piezoelectric bimorph. This is represented as a capacitor in series with a voltage source; the measured voltage is not the same as the induced voltage in the bimorph.[35] The amplitude of the measured voltage is reduced with respect to the induced voltage by a constant factor and the phase is shifted by a constant amount, both depending on the oscillation frequency and the time constant RC, where R is the equivalent resistance in the output circuit and C is the equivalent capacitance. In practice, the main contribution to the equivalent resistance of the output circuit comes from the input resistance of the measuring device. The resistance of the bimorph (>1 GΩ) is much larger than the input resistance of the measuring device ($\sim$10–100 kΩ). The equivalent capacitance C has contributions both from the capacitance of the bimorph and from the input capacitance of the measuring device. The resulting time constant, RC, is typically in the range 0.05–0.5 s.

No correction for the RC effect is needed in the calculation of the viscoelastic parameters according to the mechanical model, because the reduction factor in amplitude and the shift factor in phase cancel out in amplitude ratio and phase difference, respectively. However, in expressions where the absolute values of the amplitude are used, such as the displacement, velocity and shear rate, the RC effects had to be taken into account. RC effects are dominant at frequencies lower than $1/RC$ and the corrections can be neglected for frequencies larger than $1/RC$. RC effects can easily be corrected by calculating the voltage induced in the bimorph using the measured voltage and the measured value of the time constant according to the relation,

$$V_{\text{induced}}(t) = V_{\text{measured}}(t) + (1/RC)\int V_{\text{measured}}(t)\,dt. \quad (1)$$

An additional consideration comes into play because of tiny leakage currents due to finite resistance (though very large) of the bimorphs used. In this case, at very small output voltages (for the very smallest displacement amplitudes), smaller than 30 μV, the data has also been corrected for the offset voltage. The offset voltage is defined as the output voltage at zero input voltage. The $X = R\cos\phi$ and $Y = R\sin\phi$ components of the output voltage, where R is the amplitude and ϕ is the phase, and both are linearly related to the input voltage. When X and Y are plotted against the input voltage, the extrapolation of the linear fit to the zero input voltage are found to give nonzero intercepts of ΔX and ΔY. With decreasing input voltage, the amplitude of the output voltage then approaches to the value of $((\Delta X)^2 + (\Delta Y)^2)^{1/2}$ and the phase to $\tan^{-1}(\Delta Y/\Delta X)$. The offset voltage can be corrected by calculating the amplitude and phase after subtracting ΔX and ΔY from the X and Y components of the output voltage. The corrected amplitude, R_C, and phase, ϕ_C, are then given by

$$R_C = [(X-\Delta X)^2 + (Y-\Delta Y)^2]^{1/2}, \quad (2)$$

Downloaded 25 Jul 2001 to 130.126.103.150. Redistribution subject to AIP license or copyright, see http://ojps.aip.org/jcpo/jcpcr.jsp

$$\phi_C = \tan^{-1}[(Y-\Delta Y)/(X-\Delta X)]. \quad (3)$$

The offset voltage has a slight frequency dependence which requires the offsets in X and Y to be determined separately for each oscillation frequency. Typical values are in the range 0–3 μV.

The cleaved surface of muscovite mica has a very high surface energy. The surface energy of mica in vacuum is around 2000–4000 mJ/m^2. When cleaved in ambient air, the surface energy is an order of magnitude less, approximately 200–400 mJ/m^2, due to molecules adsorbed on to the surface. For the experiments, all the mica handling was done in ambient air and some molecules are expected to adsorb on the surface before the liquid is added. Depending on the time mica surface is exposed to the ambient air, the surface will have varying surface energies from one experiment to the other. Although this might be a source of scatter in the quantitative experimental results, no qualitative differences were observed between the experiments, all the other parameters having been kept constant. The relative cleanliness of the mica surfaces was checked by verifying the sudden jump-in when the surfaces were brought together and the jump-out when they were separated.

In some of these experiments, the cleaved mica surface was coated with a self-assembled monolayer of condensed octadecyl chains in the manner described previously.[37] The surface energy of the resulting methyl terminated surfaces is about 22 mJ/m^2, an order of magnitude less than that in ambient air, which causes a much weaker interaction of the liquid molecules with the surfaces. The experiments using such organic monolayer-coated surfaces were performed to isolate confinement effects from the effects of high surface energy and stronger molecule–surface interactions.

As the liquid sample, OMCTS (Fluka, purim grade) was used as received after control experiments showed similar behavior following further purification by distillation. Experiments were performed at 27 °C. A highly hygroscopic chemical, P_2O_5, was kept in the sealed sample chamber throughout the experiment. The sample was left in the dry chamber atmosphere for a few hours before any measurements were done. Surface separation was then decreased slowly. All the data were taken in the direction of decreasing surface separation, so that the system was always in the repulsive force regime, close to the peak of the oscillatory structural forces. Because oscillatory force amplitude increases with decreasing surface separation, below a surface separation of 4 layers it was possible to perform measurements at different increasing values of normal forces while having the same number of molecular layers between the surfaces. At larger separations the repulsive forces were weak, but the systems were transiently stable, long enough to make measurements.

The contact diameter for the thinnest films was calculated from the flattened tip of the interference fringes taking into account the lateral magnification of the focusing mechanism. However the accuracy in the measurement of contact diameter was ± 5 μm, resulting in considerable error bars for thicker films. In these instances we calculated the contact diameter with respect to the measured contact diameter of 40 μm at the maximum applied normal force of 3.81 mN, assuming a Hertzian contact. This is a reasonable assumption when one recalls that it is the glue under the mica surfaces that deforms under the action of normal pressure. The assumption was also justified empirically by the observation that these calculated contact diameters were within ± 5 μm of the measured values.

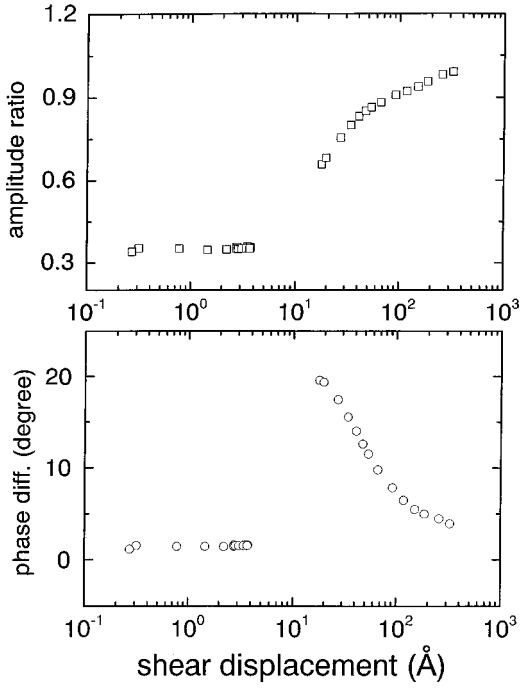

FIG. 1. Limits of linearity in an oscillatory shear experiment. OMCTS of thickness $n \approx 2$ molecular layers was deformed by oscillatory shear at 256 Hz. Amplitude ratio, the output shear voltage relative to output shear voltage for an OMCTS film of macroscopic thickness (top panel), and shear phase lag relative to an OMCTS film of macroscopic thickness (bottom panel) are plotted against shear displacement. These responses were independent of shear displacement when it is sufficiently small but deviated markedly when shear displacement exceeded ≈3 Å. The gap between shear displacements of ≈3 and ≈10 Å indicates stick-slip analyzed in detail in Fig. 2.

To analyze more quantitatively the shear forces, we also calculated the normalized forces, the effective shear moduli. For this purpose we took the elastic and viscous force constants and normalized by the effective contact area, A_{eff} and film thickness, D, to give an effect shear modulus, G_{eff}. (Here A_{eff} was estimated as described in the previous paragraph.) Specifically,

$$G'_{\text{eff}}(\omega) = [(f_{\text{elastic}}(\omega)/d)][D/A_{\text{eff}}], \quad (4)$$

$$G''_{\text{eff}}(\omega) = [(f_{\text{viscous}}(\omega)/d)][D/A_{\text{eff}}], \quad (5)$$

where the symbol, d, refers to the shear amplitude in oscillatory deformation. The elastic force constant is $f_{\text{elastic}}(\omega)/d$ and the viscous force constant is $f_{\text{viscous}}(\omega)/d$.

III. RESULTS

The goal of these measurements was very different from that in which solid surfaces are slid past one another at rapid rate to measure ''friction.'' Instead we have sought to measure the frequency dependence of linear response of confined states *unperturbed* by external shear field. When a system is

Downloaded 25 Jul 2001 to 130.126.103.150. Redistribution subject to AIP license or copyright, see http://ojps.aip.org/jcpo/jcpcr.jsp

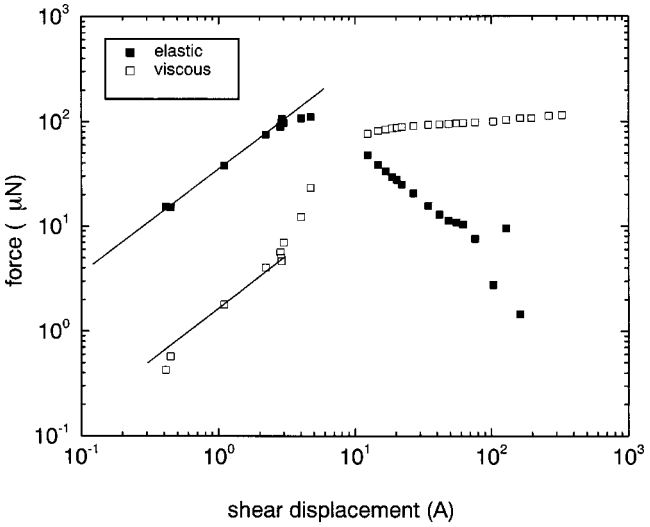

FIG. 2. Elastic and viscous shear forces calculated from the raw data in Fig. 1. At small displacements they grew in direct proportion to the shear displacement, indicating that the linear system was sheared at an oscillation amplitude small enough that the equilibrium structure of the liquid was not disturbed. In this regime, the viscoelastic parameters of the system were only a function of the oscillation frequency, not the oscillation amplitude. Filled symbols: elastic force, in phase with the shear displacement. Open symbols: viscous force, 90° out-of-phase with the shear displacement (i.e., in phase with the rate of shear displacement).

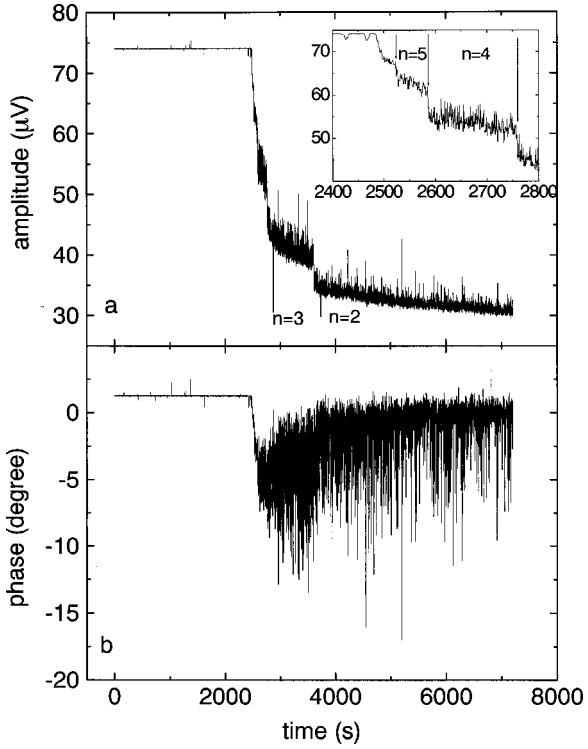

FIG. 3. Shear responses during an experiment in which mica surfaces with an OMCTS droplet came together slowly owing to thermal and mechanical drifts. The output shear voltage amplitude (top panel) and its phase (bottom panel) are plotted against elapsed time. A sinusoidal (250 Hz) applied shear force of 4.3 μN was applied (linear response regime). One observes, especially in the top panel, discontinuous changes of the shear response as successive layers of OMCTS were squeezed out. Vertical arrows show the points where a molecular layer was squeezed out from between the surfaces. The symbol "*n*" denotes the dimensionless film thickness, total film thickness normalized by the dimension of the OMCTS molecule.

sheared at an oscillation amplitude small enough that the equilibrium structure of the liquid is not disturbed, the viscoelastic parameters of the system are only a function of the oscillation frequency, not the oscillation amplitude.

A. Limits of linearity

We begin with the evidence of linearity. In general, the response of any viscoelastic system goes from linear to nonlinear with increasing oscillation amplitude.[31] Figure 1 illustrates this for the case of OMCTS deformed by oscillatory shear at 256 Hz. Amplitude ratio, the output shear voltage relative to output shear voltage for an OMCTS film of macroscopic thickness (top panel) and shear phase lag relative to an OMCTS film of macroscopic thickness (bottom panel) are plotted against shear displacement.

The abscissa is peak shear displacement during the oscillatory cycle. The phase and amplitude ratio were independent of shear displacement provided that this was sufficiently small but deviated markedly when the shear displacement exceeded ≈3 Å. Beyond this point of "slip" the sliding surfaces accelerated to keep up with the applied force. Consequently the shear displacement increased discontinuously from ≈3 to ≈10 Å. The large phase lag in this sliding regime is symptomatic of predominantly dissipative deformation (kinetic friction). However, in the linear region, the moderate phase lag and small amplitude ratio are symptomatic of "solidification." It will be shown below that they can be used to quantify the stiffness of the "solid" state.

Alternatively, the same data can be expressed as elastic and viscous force, as shown in Fig. 2. This is done by expressing the shear response as one part in phase with the shear displacement (the elastic force) and one part in phase with the rate of shear displacement (the viscous force). For sufficiently small displacements both forces grew in direct proportion to the shear displacement, indicating that the linear system was sheared at an amplitude small enough that the equilibrium structure of the liquid was not disturbed. When the elastic force reached a critical level the elastic energy stored could no longer withstand the forcing shear and the system broke apart. The peak elastic force, which corresponds to the static friction in this system, has been analyzed in detail by us previously.[34] The subsequent kinetic friction is nearly independent of shear displacement per unit time, i.e., is nearly independent of effective velocity.[34,38] In this paper we are concerned with stiffness in the "stick" region.

B. Thickness dependence of viscoelastic parameters at constant oscillation frequency

The effect of the film thickness on the viscoelastic parameters was observed by letting the surfaces slowly drift into contact while a constant shear force was applied to one of the shear bimorphs at a constant oscillation frequency. Due to thermal and mechanical drifts, the surface separation decreased with time until a single molecular layer was left between the surfaces.

Figure 3 shows typical raw data, namely, the amplitude (top panel) and the phase (bottom panel) of the output volt-

Downloaded 25 Jul 2001 to 130.126.103.150. Redistribution subject to AIP license or copyright, see http://ojps.aip.org/jcpo/jcpcr.jsp

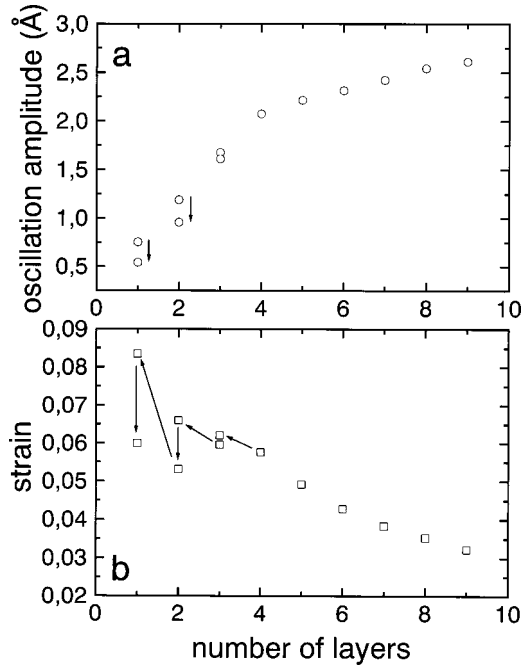

FIG. 4. Shear displacements (top panel) and strain, the ratio of shear displacement to film thickness (bottom panel), plotted against the number of confined molecular layers for the same OMCTS/mica system whose raw data are presented in Fig. 3. The arrows indicate the direction of increasing time. One observes that the confined liquid film grew progressively stiffer as it became thinner. Note that even at the same number of molecular layers, the oscillation amplitude and the strain decreased in time because the normal pressure on the system increased from thermal and mechanical drifts. This caused a small decrease in the surface separation, too small to measure with the few Å resolution of the optical technique employed to measure surface separation, but still significantly affecting the shear oscillation amplitudes. These time effects were especially clear when there were few molecular layers of OMCTS between the surfaces.

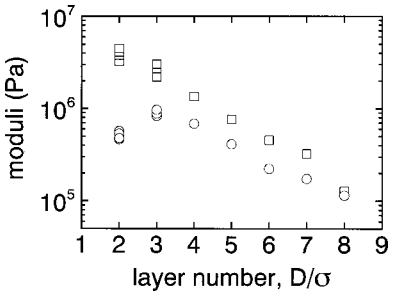

FIG. 5. Effective shear moduli calculated from the raw data shown in Figs. 3 and 4. The storage modulus G' (squares) and loss modulus G'' (circles) are plotted as a function of the number of molecular layers for the OMCTS/mica system, quantifying how the confined film grew progressively stiffer at it became thinner.

age, plotted against time as the surfaces drifted in and the film thickness decreased. The applied shear force amplitude was kept constant at 4.3 μN and the oscillation frequency was 250 Hz. The discontinuous changes in the shear amplitude and phase, indicated by arrows in Fig. 3, were due to a molecular layer being squeezed out of the surfaces. The film thickness in number of molecular layers is also shown in the figure. The onset of confinement effects was at $n=8$; at larger film thickness there was no discernible difference from bulk response.

With decreasing film thickness, first both the amplitude and the phase of the output voltage decreased. At a film thickness of $n=3$ the phase passed through a minimum and started increasing while the amplitude continued decreasing. Such behavior of amplitude and phase indicate an increasing elasticity with decreasing film thickness and imply that the frequency-dependent viscosity peaks (at this frequency) at the film thickness where the phase is minimum.

Increased fluctuations of amplitude and phase with decreasing film thickness are due to two factors. First, the signal to noise ratio decreases with decreasing amplitude. Second, the critical shear rate decreases and the system comes closer to the linear/nonlinear boundary. The significant fluctuations observed at film thickness smaller than $n=3$, even at oscillation amplitudes as small as 1–2 Å, were mainly due to the system being close to the linear/nonlinear boundary. We have discussed such fluctuations elsewhere.[39] Although the exact form of the curve for the amplitude and phase depends on the oscillation frequency, the above qualitative observations are common to any frequency within our experimental frequency window.

In these experiments the applied force was kept constant. Therefore, as the films became stiffer, the shear oscillation amplitude decreased with decreasing film thickness. Figure 4 (top panel) shows the oscillation amplitude as a function of film thickness in number of molecular layers between the surfaces for an applied force of 4.3 μN at 250 Hz. The oscillation amplitude decreased approximately by a factor of 4 as the film thickness decreased by a factor of 8.

It is convenient to express this in terms of a dimensionless number, defined as shear displacement normalized by film thickness, the ''strain.'' The strain was approximately doubled as the surfaces drifted in till a single molecular layer was left between the surfaces, as shown in Fig. 4 (bottom panel). The arrows indicate the direction of time. Even at the same number of molecular layers, the oscillation amplitude and the strain decreased in time because the normal pressure on the system increased due to thermal and mechanical drifts. This caused a small decrease in the surface separation—too small to be measured with the few Å resolution of the optical technique to measure the surface separation, but still significantly affecting the oscillation amplitude. These time effects were especially clear when there were few molecular layers of OMCTS between the surfaces.

The important question is whether, in Fig. 4 (bottom) the maximum strain of 0.07, corresponding to a shear rate of 110 rad s^{-1} at 250 Hz, was still in the linear response regime or not. The dependence of the critical shear rate on the film thickness is difficult to quantify, especially in the liquidlike regime. If one intuitively assumes that the longest relaxation time of the system monotonically increases, decreasing the critical shear rate, with decreasing film thickness, a thickness will be reached where the shear rate will exceed the critical shear rate and the system will go into the nonlinear region. Even if the response does not become nonlinear, it is definite that the system gets closer to the linear/nonlinear boundary with decreasing film thickness and some slight changes in the response are not unusual. In the solidlike regime, the

Downloaded 25 Jul 2001 to 130.126.103.150. Redistribution subject to AIP license or copyright, see http://ojps.aip.org/jcpo/jcpcr.jsp

transition from linear response to non-linear response happens when the structure yields (as illustrated in Fig. 2). The yield stress and the yield strain significantly depend on the normal pressure.

Plotted as a function of the film thickness expressed in number of molecular layers, Fig. 5 shows the storage modulus, G', and the loss modulus, G'', calculated from the raw data of Fig. 3. Here G' is the component of the resulting stress normalized by the strain that is in phase with the applied stress and G'' is the component of the resulting stress normalized by the strain that is out of phase with the applied stress. The area, A, calculated from the optically measured contact diameter, D, using $A=(\pi/4)\cdot(D/M)^2$, where M is the magnification of the optics, was constant at 102 μm^2 for all these measurements. At 250 Hz, the crossover from a predominantly viscous response ($G'<G''$) to a predominantly elastic response ($G'>G''$) happened at a film thickness larger than $n=8$ and G' is larger than G'' at every film thickness in Fig. 5. At lower frequencies, this crossover happened at lesser film thickness and could be observed. However, in no case was there observed an abrupt change in the dependence of moduli on the film thickness. The data taken at every frequency showed the common pattern that moduli increased, roughly exponentially with diminishing film thickness until G' leveled off and G'' passed through a maximum.

The structural changes that take place under confinement and whether a phase transition is involved in the confinement-induced solidity of liquids have been of controversy,[9–14] as already noted. The observations presented so far amount to the first piece of evidence that an abrupt transition does not occur.

The maximum in G'' at a film thickness of $n=3$ is clearly seen in Fig. 5. This tells that the maximum dissipation happens at a film thickness of $n=3$ at 250 Hz. Experimentally, it is difficult to observe the position of the maximum with changing frequency due to insufficient thickness resolution. Instead, the frequency dependence of the moduli at constant film thickness will be observed as discussed in the next section. Thickness dependence of moduli at constant frequency and the frequency dependence at constant film thickness will be related to one another in the following section.

C. Thickness dependence of the frequency spectrum

The significance of linear response in oscillatory shear experiments is that it provides a way to study molecular motions in confined liquids without disturbing the equilibrium structure of the liquid. The oscillation frequency introduces a time scale $\tau_1 \sim 1/\omega_1$, where ω_1 is the frequency where $G'=G''$. Molecular motions with relaxation times shorter than τ_1 are barely affected by the shear, while those with longer relaxation times are strongly influenced. The frequency spectrum of the storage and loss modulus is important as it is possible to relate the maxima of the moduli to particular types of molecular motion in the liquid. The maximum in the loss modulus, a measure of energy dissipated or lost as heat per cycle of sinusoidal deformation, can be regarded as a ''damping'' effect and occurs at the frequency of some molecular motion in the liquid structure. At higher frequencies there will be insufficient time for the molecules to relax the stress imposed by shear and the material will be relatively stiff. On the other hand at lower frequencies the molecules will have more time to move and the liquid will appear to be soft.

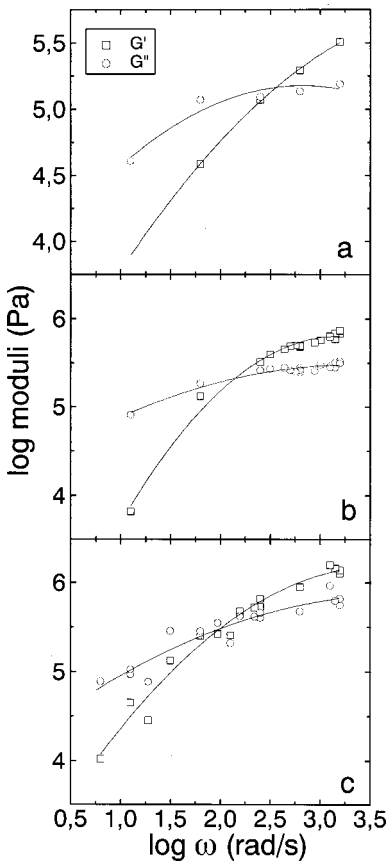

FIG. 6. The shear frequency spectrum for the OMCTS/mica system at different film thicknesses: (a) $n=7$; (b) $n=5$; (c) $n=4$, where n is dimensionless film thickness, total film thickness normalized by thickness of the OMCTS molecule. The solid lines are second order polynomial fits to the data. The elastic modulus G' is denoted by squares, and the viscous modulus G'' by circles.

The major experimental challenge to get the frequency spectrum of the moduli, especially at larger film thickness, was to keep the system stable at a constant surface separation. Due to thermal and mechanical instabilities, the data at large film thicknesses had to be taken within a few minutes. This did not allow more than several different frequencies to be applied and the data were averaged for a shorter time interval than otherwise. At smaller film thickness, the scatter in the data came from the larger range of amplitude and phase for a given thickness. As time passed the amplitude and the phase changed due to increasing normal pressure although the measured film thickness was constant, giving a slightly different frequency spectrum for the same thickness.

Figure 6 shows the storage modulus, G', and the loss modulus, G'', of an OMCTS film as a function of frequency at film thickness corresponding to (a) $n=7$; (b) $n=5$; and (c) $n=4$. The solid lines are the polynomial fits to the data to guide the eye and to be used in determining the crossover frequency from predominantly viscous to elastic behavior. At low frequencies, shear induced perturbations were relaxed by

Downloaded 25 Jul 2001 to 130.126.103.150. Redistribution subject to AIP license or copyright, see http://ojps.aip.org/jcpo/jcpcr.jsp

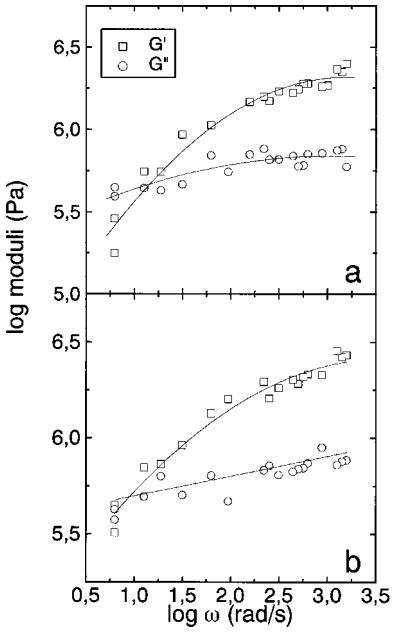

FIG. 7. Effect of increasing normal pressure on the shear frequency spectrum of the OMCTS/mica system at a film thickness of $n=3$. The data in the bottom panel, taken after the data in the top panel, show a slower terminal relaxation time, reflecting the higher normal pressure. The shear data were acquired at 250 Hz under a shear force of 4.3 μN. The elastic modulus G' is denoted by squares, the viscous modulus G'' by circles.

molecular motions that dissipate energy and the film was predominantly viscous. At higher frequencies, the perturbations could no longer be relaxed in the period of the oscillation resulting in energy storage and hence an increase in the elastic component. The general trend in the frequency dependence above and below the crossover frequency is difficult to conclude from such data because of limited number of data points above and below the crossover frequency.

The viscoelastic frequency spectra in Fig. 6 are typical of liquids in a frequency range near $1/\tau_1$, the inverse terminal relaxation time. The films relaxed shear stress predominantly in the manner of viscous liquids when the frequency was less than $1/\tau_1$; at high frequencies the perturbation was not relaxed during the period of oscillation and energy was stored. From common experience, the analogous viscoelastic phenomenon is known for silly putty: it bounces when dropped on a floor (high-frequency response) but flows when it sits on a table.

From the intersection of the polynomial fits shown as solid lines in Fig. 6, the crossover frequency was found as 56.0 Hz for $n=7$ thick film, 22.2 Hz for $n=5$, and 15.6 Hz for $n=4$. It is clearly seen that crossover frequency shifted to lower frequencies as the film thickness decreased. This shift to lower frequencies indicates slower relaxation dynamics. If the film thickness is further decreased, the crossover frequency moved further down in the frequency.

The effect of normal pressure at constant film thickness is illustrated in Fig. 7. Figure 7 (top and bottom panels) are the frequency spectra of an OMCTS film of thickness $n=3$. The data in the bottom panel were taken after those in the top panel. The crossover frequency is found to be 2.4 Hz for the top panel and 1.1 Hz for the bottom panel. Here it is

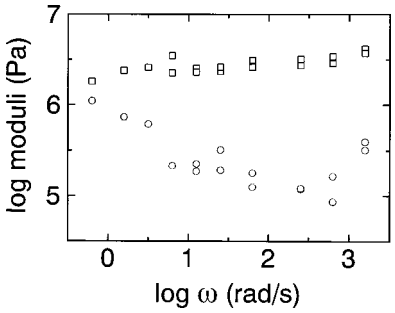

FIG. 8. The shear frequency spectrum of the OMCTS/mica system at a film thickness of $n=1$. The elastic modulus G' is denoted by squares, the viscous modulus G'' by circles.

seen that though the film thickness was constant within the experimental uncertainty of 1–2 Å, the relaxation dynamics slowed and the crossover frequency continued to move to lower frequencies. Because the oscillation amplitude was small enough not to disturb the equilibrium structure strongly, this change in the frequency spectrum towards slower relaxation was due to increase of normal pressure on the system because of thermal and mechanical drifts. As the pressure increased, the state of the system climbed up the repulsive side of a peak in the force-distance profile. This thickness change is not possible to observe with the few angstrom resolution of our technique. However, such a small change has a significant effect on the relaxation dynamics. For a constant number of layers between the surfaces, this slowdown in molecular motions could qualitatively be understood in terms of the free volume, which is the space available for the molecules to move between the surfaces. With the contact area being constant, the free volume decreased with decreasing surface separation and the molecular motions slowed down because it became more difficult for the molecules to find empty spaces to jump into.

Figure 8 shows the frequency spectrum for an OMCTS film of thickness $n=1$. The crossover of the storage and loss modulus in this case did not happen within the frequency window. Contrary to the frequency dependency in Figs. 6 and 7, here G'' decreased with increasing frequency and the frequency dependence of G' was less, though still increasing slightly with increasing frequency. The crossover frequency was found to be 0.11 Hz as determined from the intersection of the polynomial fits to the data. To estimate the crossover frequency by extrapolating the fits to the data may be justified, so long as the crossover is not far from the lower limit of the frequency window, and the estimated value follows same trend in thickness dependence set by the previous measurements where the crossover frequency was within the experimental frequency window. As will be clear in the next section, the estimated crossover frequency falls, by coincidence, on the same thickness dependence curve determined by the previous measurements at larger film thickness. Of course the actual data points would not follow the polynomial fits below the frequency window, if data were taken at the lowest frequencies.

From the general trend of the frequency spectra with

Downloaded 25 Jul 2001 to 130.126.103.150. Redistribution subject to AIP license or copyright, see http://ojps.aip.org/jcpo/jcpcr.jsp

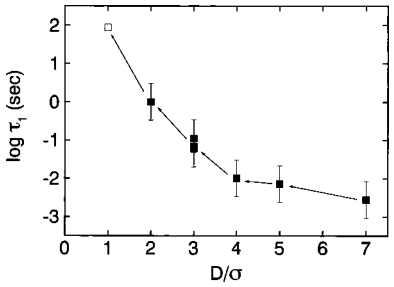

FIG. 9. Terminal relaxation time, τ_1, plotted logarithmically against film thickness expressed in multiples of the molecular dimension of OMCTS. Data at different thickness were acquired by squeezing the surfaces together progressively (data for $D/r=6$ are missing owing to thermal drifts). Open square: extrapolated τ_1 used for frequency-thickness superposition shown in Fig. 10. Filled squares: measured values.

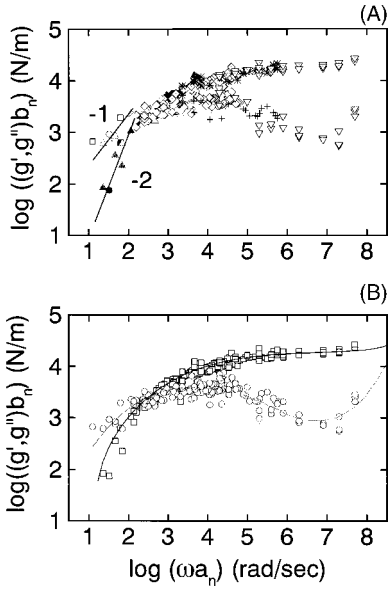

FIG. 10. Master curve describing frequency-thickness superposition of the viscoelastic response. The shear moduli were normalized by h_n/A with respect to a film thickness of $n=7$ molecular dimensions. The g' and g'' are the elastic and viscous shear forces, respectively, normalized by shear displacement (≈ 2 Å). The reference state is $n=D/\sigma=7$ molecular layers. Data at other film thickness were shifted vertically (shifts denoted b_n) and horizontally (shifts denoted a_n) as described in text, to make the elastic and dissipative spring constants coincide at x_c. (Panel A): The following symbols indicate real and imaginary components, respectively: filled and open squares ($D/\sigma=7$); filled and open circles ($D/\sigma=5$); filled and open triangles to right ($D/\sigma=4$); diamonds with and without center dot ($D/\sigma=3$); stars and plus sign ($D/\sigma=2$); triangles with and without center dot ($D/\sigma=1$). The logarithmic slopes of $+1$ and $+2$ are the classical response of a fluid dictated by the Kramers–Kronig relations. (Panel B): Imaginary component (bottom curve) calculated from the real component (top curve) using the Kramers–Kronig relation. Line through the top curve is a third order polynomial fit to the data. Data taken at different D/σ are identified in Panel A.

decreasing film thickness as shown in Figs. 6, 7, and 8, it is clear to see that within the frequency window of 1–260 Hz, the storage modulus flattened, i.e., became less dependent on frequency, with decreasing film thickness. The positive frequency dependence of the loss modulus decreased, became negative and then formed a minimum. The magnitudes of the storage and loss modulus increased with decreasing film thickness while the crossover frequency shifted to lower values. Can we conclude anything from this data about the larger frequency window behavior of the frequency spectrum? Could the frequency spectrum taken at different film thickness be related to each other and form a general picture in the frequency-thickness domain? The answers to these questions will be discussed in the next section.

These raw data show definitively that the change of viscoelastic response was continuous rather than abrupt with decreasing film thickness. To quantify τ_1, a useful measure was the inverse frequency at which the ratio of dissipative and elastic force was unity. In Fig. 9, τ_1 is plotted semilogarithmically against film thickness expressed as multiples of the molecular diameter of OMCTS. The sudden slowing down of τ_1 by three orders of magnitude, as the film was squeezed from a thickness of 7–2 molecular dimensions, is striking. Though the limited range of thickness admits various functional fits, the increase of τ_1 appears to more rapid than exponential. Well-known viscoelastic relations show that the effective viscosity of a viscoelastic body is proportional to τ_1,[31] indicating a similarly sudden increase of the viscosity. Control experiments confirmed this result also for confinement between noncrystalline surfaces, between mica coated with a densely-packed self-assembled monolayer of octadecyl chains terminated with methyl groups.[35]

The dependence on sample history was consistent with the hypothesis of a glassy state. This is quantified in the large error bars in Fig. 9. The error bars exceed the experimental uncertainty. In repeated experiments, variations of the compression rate resulted in somewhat different τ_1 at a given film thickness. If liquid exchange between the confined volume and the reservoir outside were suppressed by the sluggish mobility upon confinement, molecules might become trapped within the gap when the solid surfaces were squeezed together rapidly.

D. The shear stiffness is "soft"

When assessing the hypothesis of confinement-induced crystallization, it is worth emphasizing that the elastic rigidity measured in these experiments in the rest state, g_c' was low. Here g_c' is the elastic stiffness, the linear elastic force normalized by shear displacement in the regime at frequencies where g' is nearly independent of ω. The effective contact area between curved surfaces in this experiment is on the order of 10 μm in diameter. Dividing by area and multiplying by thickness gives the frequency-dependent elastic shear modulus, whose units are energy per unit volume.

From this reasoning, it follows that the volume attributable to a k_BT of elastic energy ranged from ≈ 30 molecules (at thickness of 7 molecules) to ≈ 6 molecules (thickness of 2 molecules). Clearly, explanation should not be sought in single molecule–molecule interactions, but rather in collective interactions at larger length scales than molecular—again consistent with the hypothesis of glassy response.

This weak stiffness also helps to explain why it is possible to pass sequentially to smaller-and-smaller film thickness simply by applying increasing compressive force to a confined liquid—a transition that would not be feasible to effect in the case of an ordinary macroscopic crystal.

Downloaded 25 Jul 2001 to 130.126.103.150. Redistribution subject to AIP license or copyright, see http://ojps.aip.org/jcpo/jcpcr.jsp

E. Time-thickness superposition

A general interpretation of the above linear data for a constant film thickness is difficult due to the relatively small frequency window. On the other hand, the method of reduced variables has long been used as a means for enlarging the effective time or frequency scale available for experimental measurements. In this section, we apply this method to the linear data of the previous section to see if it results in separating the two principal variables of time (or frequency) and thickness on which the viscoelastic properties depend. In such a case, the properties can be expressed in terms of a single function of each variable, whose form can be determined experimentally whether or not it can be conveniently represented by an analytical expression.

In Ref. 31, three criteria have been listed for the applicability of the method of reduced variables. (i) Exact matching of the shapes of adjacent curves over a substantial range of frequencies. (ii) The same values of the shift factor a_T must superpose all the viscoelastic functions. (iii) The temperature dependence of a_T must have a reasonable form consistent with experience. When a_T is a smooth function of temperature with no gross fluctuations or irregularities, it is usually fitted to the WLF expression. For the time-thickness superposition presented here, the above criteria will also apply with slight modifications, the major one being the replacement of temperature with thickness.

The viscoelastic spectra measured at different film thickness were shifted on log–log scales so as to coincide at the crossover frequency, ω_c, where $G'=G''$. Figure 10 (top panel) shows the resulting composite graph. This master curve consists of data taken at six different levels of film thickness but shifted on both the horizontal and vertical scales to coincide at $\omega=\omega_c$. The linear response data fell on a single curve, within experimental scatter, in a frequency range of more than six orders of magnitude when superposed along the lines outlined below, with a few exceptions (discussed in the fourth paragraph below) for the shift factors of $n=1$ and $n=2$ thick films. Specifically, the elastic and viscous spring constants are plotted against frequency on log–log scales. The reference state is the film of thickness $n=D/\sigma=7$ molecular dimensions. For films of lesser n, the data are shifted on the frequency scale by $a_n=\tau_1(n)/\tau_1(7)$. On the vertical scale, they are shifted by $b_n=g'(1/\tau_1(n)/g'(1/\tau_1(7))$. A viscoelastic property measured at frequency ω and a given thickness was equivalent to the same viscoelastic property measured at a different frequency ωa_n and different thickness n.

This is a generalization of the horizontal shift factor to give the ratio a_{12} of a particular relaxation time τ in state 2 to that in state 1 in conventional time-temperature superposition.[31] For the case of time-thickness superposition, the horizontal shift factor a_n is then given by the ratio of the relaxation time τ_n at a film thickness of n molecular layers to τ_{n0} at n_0 molecular layers. A relaxation time, τ, for the system is defined as the reciprocal of the crossover frequency, ω_c. This means that all the curves have to be shifted horizontally with respect to a reference curve in such a way that the crossover frequencies are all at the same point on the horizontal axis.

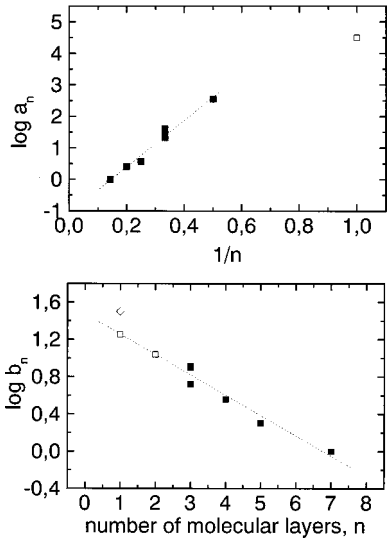

FIG. 11. The horizontal (top panel) and vertical shift factors (bottom panel) plotted semilogarithmically against reciprocal of layer number (top panel) and against layer number (bottom panel). The dotted lines are exponential fits to the data. The filled (open) squares were determined experimentally (empirically). The datum represented by a diamond corresponds to ~1 MPa more external pressure than the datum represented by the square. Here the vertical shift factor is the relative elastic spring constant of confined OMCTS at the frequency (ω_c) where elastic and dissipative shear forces are equal. The elastic spring constant is the measured elastic shear force normalized by shear displacement. The horizontal shift factor is the relative terminal frequency (ω_c) where elastic and dissipative shear forces are equal.

The vertical shift factors b_n are based on the hypothesis that the magnitude of the modulus G_c at the crossover frequency normalized by D_n/A_{eff} should be the same for all the superposed data.

The superposition of the data using the shift factors a_n and b_n as described above is then equivalent to frequency spectra at different film thickness being pinned down at the intersection of the AG'_{eff}/D_n and AG''_{eff}/D_n curves. This is an advantage obtained by simultaneous measurement of G' and G''. Explicit values of the horizontal and vertical shift factors are plotted against layer number in Fig. 11.

It has to be emphasized that this way of determining the shift factors does not bring any arbitrariness into the method, since everything is, in principle, determined from experimentally measured values. However, slight modifications from the experimentally-determined values were used for the films of thickness $n=2$ and $n=1$. Although the a_n value that was determined from the crossover by extrapolating the polynomial fits in Fig. 8 was used for $n=2$ thick film, $\log b_n=1$ was used instead of $\log b_n=1.367$ as determined from the crossover, so that b_n continued to satisfy the analytical expression which increases exponentially with decreasing film thickness, $\log b_n=1.42-0.21n$, and was determined by the crossover points for $n>2$. Vertical shift factors of 1.21 and 1, as calculated from the above expression, were used for the data of $n=1$ and $n=2$ thick films, respectively. A vertical shift factor of $\log b_n=1.44$ was used to superpose the data of 1 ML thick film taken after applying a normal external pressure of approximately 1 MPa. The effect of normal pressure will be discussed below. An empirical horizontal shift factor of $\log a_n=4.5$ was used for all data corresponding to $n=1$

Downloaded 25 Jul 2001 to 130.126.103.150. Redistribution subject to AIP license or copyright, see http://ojps.aip.org/jcpo/jcpcr.jsp

thick films, although it did not fall on the line, $\log a_n = (7.88/n) - 1.19$, determined by the crossover frequencies for $n > 1$ and showing the linearity of $\log a_n$ to $1/n$. The above expression gives a value of $\log a_n = 6.69$ for $n = 1$ which does not enable the superposition of the data for 1 ML thick films. The thickness dependence of a_n and b_n will be discussed in detail below.[40]

The consistency of the interrelation between the storage and loss moduli was checked through Kramers–Krönig relation. One approximate expression relating the values of G' at two frequencies ω_1 and ω_2 is given as[31,41]

$$G'(\omega_2) - G'(\omega_1) \cong (2/\pi) \int (G''(\omega) d(\ln \omega)). \tag{6}$$

To check whether the master curve in Fig. 10 (top panel) satisfied this relation, a third order polynomial was fitted, $A_0 + A_1(\ln \omega) + A_2(\ln \omega)^2 + A_3(\ln \omega)^3$, to AG''_{eff}/D_n data with the fitting parameters $A_0 = 0.312$, $A_1 = 1.759$, $A_2 = -0.386$, and $A_3 = 0.027$, shown as the solid line through $g'(\omega)$ in the bottom panel of Fig. 10. The integration of this curve between the lower and the upper limits of the frequency window over more than six decades, multiplied by $(2/\pi)$, gave the line through $g''(\omega)$ in the bottom panel of Fig. 10. This fits the data over most of the frequency window, except at frequencies below the crossover of g' and g''. At the lowest frequencies the curve gives somewhat larger values than the actual data points. The good consistency of the approximate Kramers–Krönig relation with the actual superposed data over almost six decades is one check for the trustworthiness and self-consistency of this method of reduced variables.

IV. DISCUSSION

The confinement-induced solidity of liquids has been known since the late 1980s.[1,2] However, the nature of this transition has been controversial. In one point of view, it was suggested that this is a first-order phase transition where above a critical film thickness the system is purely viscous and below that it is purely elastic, as discussed in the Introduction. The frequency spectrum of the superposed data suggests instead a physical picture in terms of a gradual transition to a predominantly elastic state similar to the glass transition of low molecular weight liquids with decreasing temperature.[31] Also supporting this interpretation is the gradual increase, with decreasing film thickness, of the relaxation time and of the magnitudes of the viscoelastic moduli.

A. Split between two families of relaxation times

The preceding section has presented a phenomenological master curve that appears to succeed in superposing the data. The key point is wide separation between two families of viscoelastic relaxation. Figure 10 shows a broad maximum in $g''(\omega a_n)$ at low reduced frequency, indicating one cluster of relaxation times. At much higher reduced frequency the $g''(\omega a_n)$ rise sharply, indicating the onset of additional relaxation processes. It is curious that these two clusters of relaxation times seem to be separated by a constant distance on the reduced frequency scale. This constitutes an important difference from the well-known α and β relaxations of bulk glasses, whose separation increases with increasing pressure or diminishing temperature.[29,42] A point for future work will be to expand the experimental frequency window to better probe the relaxation processes at high ωa_n, to test more strictly whether the observed frequency-thickness superposition will hold as well at high frequency as at low. This, however, is not yet feasible with our present experimental setup.

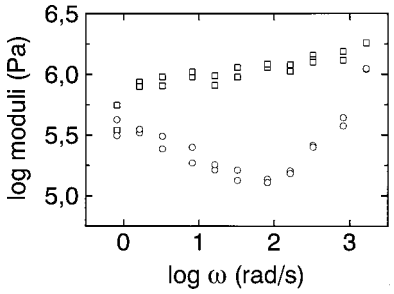

FIG. 12. The shear frequency spectrum of the OMCTS/OTE/mica system at a film thickness of $n = 1$. The elastic modulus G' is denoted by squares, the viscous modulus G'' by circles.

For the data in Fig. 10, the loss modulus peaks at a reduced frequency of approximately $10^4\,\mathrm{rad\,s^{-1}}$ and has a clear minimum around $10^6\,\mathrm{rad\,s^{-1}}$ indicating the possibility of a second set of relaxation times peaking above a frequency of $10^8\,\mathrm{rad\,s^{-1}}$.

A phenomenologically-similar minimum in $G''(\omega)$ has also been observed for colloidal hard sphere suspensions close to the glass transition[43,44] and interpreted as having two sets of widely separated relaxation times. Having two sets of relaxation times are also well known in the case of other glass formers.[42,45] Although the molecular interpretation of the responsible relaxation mechanisms might depend on the specific system in question, for the glass transition of small molecules it is generally agreed that the faster relaxation is due to the localized motion of individual molecules in the cages formed by neighboring molecules and that the slower relaxation is associated with the breakup of these cages. Under extreme confinement, high densities are expected and similar mechanisms might be responsible in the relaxation of thin liquid films. While only the broad peak corresponding to the slow relaxation associated with the break up of cages is seen in our data, the fast relaxation is only suggested in this data by the tendency of the loss modulus to increase at the highest frequencies.[46]

As in the case of time–temperature superposition principle, the successful superposition of all the linear data onto a master curve evokes free volume arguments. Does the mobility at any film thickness depend primarily on the free volume remaining? Can the relaxation times be expressed in terms of fraction of free volume rather than the film thickness as the independent variable? What is the significance of the interactions of the molecules with the surface and with other molecules? Although successful superposition of the data might suggest, along the lines of physical explanation of WLF equation in terms of free volume, that the free volume governs the relaxation times of confined liquids, the relative

Downloaded 25 Jul 2001 to 130.126.103.150. Redistribution subject to AIP license or copyright, see http://ojps.aip.org/jcpo/jcpcr.jsp

importance of molecule–surface interactions is intuitively expected to increase with decreasing film thickness.

B. Contrast between mica and methylated mica surfaces

The significance of the energy of solid surfaces on the relaxation dynamics of the confined liquids can be experimentally understood by repeating the experiments with solid surfaces of different energies. A procedure was previously introduced[37] to modify high energy mica surfaces with octadecyltriethoxysilane (OTE) monolayers. The resulting methyl terminated surfaces have surface energies of ~ 22 mJ/m^2, approximately an order of magnitude less than the surface energy of mica cleaved in ambient atmosphere, and these surface lack long-range crystallinity. At a given film thickness, the linear shear response of OMCTS confined between OTE coated mica surfaces was more viscous compared to that between mica surfaces. However, the system eventually went into predominantly elastic state at a film thickness of $n=1$. Elsewhere we show that the successful application of these same methods of time-thickness superposition.[42] Figure 12 shows the frequency dependence of storage and loss modulus in this elastic state. Qualitatively it looks very similar to Fig. 8 showing the frequency dependence in the elastic state of OMCTS confined between mica surfaces.

However a more extensive study of this problem shows that the peak of $G''(\omega)$ spans, in the case of OMCTS confined between methylated mica surfaces, occupies a smaller span of ω than for the case of bare mica surfaces.[42] In other words, the relaxation peak at low frequency corresponds, for methylated mica, to a more narrow distribution of relaxation times. This is consistent with the intuitive expectation that weaker surface adsorption might result in a more homogeneous confining environment.

C. The independent variable: Thickness or normal pressure?

So far in this discussion, the film thickness in number of molecular layers between the surfaces was used as the independent variable, as this could be measured most readily. However, in the way that the experiment is performed, film thickness adjusts to the action of force in the normal direction. The associated surface separation D for a film thickness of n molecular layers spans a range approximately from $n\sigma$ to $(n+1/2)\ \sigma$, where σ is the molecular diameter. The approximate range of $(n+1/2)\sigma < D_n < (n+1)\sigma$ is not accessible because of the finite spring constant of the force transducer (a double cantilever spring). Considering that σ is approximately 9 Å for OMCTS, a resolution of 2–3 Å in the measurement of the surface separation easily allows to assign the number of molecular layers between the surfaces. However, the assignment of the exact surface separation is quite difficult given the range of $\sigma/2$–4.5 Å.

Since pressure is a single-valued function of the surface separation, the surface separation can be considered as the independent variable. However, experiments are done at constant pressure and surface separation can change, although no change in surface separation is expected in the linear response regime where the oscillation amplitudes are small. Differences between constant pressure and constant volume experiments (constant surface separation assuming the contact area is constant) were investigated by computer simulations.[23,45] Experimentally there are difficulties in doing a systematic study of the effect of pressure at constant film thickness or the film thickness at constant pressure. The computer simulations[23] show that the viscosity and the longest relaxation time of the confined liquids increase with decreasing film thickness at constant pressure and with increasing pressure at constant number of layers between the surfaces as expected intuitively.

For a given number of layers between the surfaces, the use of pressure as the independent variable is more reasonable. The moduli are then a function of the total pressure which is a sum of internal and external contributions. Internal pressure is related to the free energy, $F(D)=U(D)-TS(D)$, by $P_{\text{int}}=-1/A(dF/dD)_{T,N}$. The moduli increases with increasing total pressure. At constant number of molecular layers between the surfaces and for a given surface energy, the change in the moduli is dominantly due to externally applied pressure assuming that the change in the internal pressure is small because of the small change in the surface separation. On the other hand, using different surfaces and thus changing the surface energy only effects the internal pressure. The external pressure is effected indirectly because the force-distance profile and thus the range of external pressure that can be applied at that film thickness changes.

In Fig. 12, the magnitudes of the viscoelastic moduli are less than expected by extrapolating from Figs. 7 and 8 for the OMCTS/mica system. Decreasing the surface energy by an order of magnitude decreases the internal pressure and thus the internal energy. So the elasticity and the shift factor go down.

V. CONCLUSIONS

In summary, the available shear experiments show that the transition towards progressively more sluggish relaxation, with increasing confinement, is more reminiscent of a glass transition than a first-order process. With increasing normal pressure, time, or increase of confinement, a viscous state evolves to a solidlike state in which the elastic forces exceed the viscous forces at a given frequency or rate of deformation. This is reminiscent of a glass-forming liquid, in which a very sharp enhancement of viscosity is observed at the glass transition, eventually appearing as a glass over the time scale of the experiment.

These conclusions, initially based on study of simple hydrocarbon liquids[5] and later on studies with OMCTS, a globular-shaped liquid,[3,15] are further supported by the fact that even glass-forming polymeric liquids without a melting transition show a similar solidlike behavior upon extreme confinement.[32,33]

For bulk fluids, an extremely small change of density leads to these large changes of viscosity. While it is true that the behavior of confined fluids is reminiscent of this as concerns sensitivity to film thickness and pressure, the clear rea-

Downloaded 25 Jul 2001 to 130.126.103.150. Redistribution subject to AIP license or copyright, see http://ojps.aip.org/jcpo/jcpcr.jsp

son for the observed slowing down of dynamics under extreme confinement is not yet fully understood.

However, recent studies have argued that OMCTS and other small-molecule nonpolar liquids, upon confinement from 7 to 6 molecular layers between mica surfaces, undergo a confinement-induced phase transition from a liquid, with viscosity close to the bulk, to a solid.[12–14] It was argued that the transition is abrupt, with a change of effective viscosity of at least seven orders of magnitude when the film thickness is reduced by the spacing of one diameter. This contrasting conclusion has motivated us to re-evaluate the current instrumentation and interpretative analysis available in various laboratories. This is contained in the Appendix.

ACKNOWLEDGMENTS

The authors are indebted to Lenore Cai, Ali Dhinojwala, Jack F. Douglas, Jacob Klein, Mark O. Robbins, and Kenneth S. Schweizer for discussions. This work was supported by grants from the Ford Motor Company and the Department of Energy through the Frederick Seitz Materials Research Laboratory at the University of Illinois. For travel assistance, the authors are grateful to TUBITAK (in Turkey) and to the U.S. National Science Foundation (International Programs).

APPENDIX: COMPARISON BETWEEN DYNAMIC SHEAR FORCE MEASUREMENTS IN DIFFERENT LABORATORIES

A version of the discussion that follows has appeared previously.[46]

1. Resolution in measuring viscosity

There exist two different approaches to measure shear forces. The first is to infer force as a surface is translated at a steady velocity (or alternatively to hold a surface constant and measure force after cessation of shear translation).[2,12,13] The second approach is to apply a small sinusoidal shear displacement force and to measure the resulting phase and amplitude of motion.[1,9,10] In the latter case there exist both elastic and viscous contributions, as discussed in the Experiment. The elastic contribution (k) is in phase with the displacement and the viscous contribution (ωb) is 90° out of phase. These are determined by the following relations:[35]

$$k = k_s[(v_f/v_c)\cos\varphi - 1], \tag{A1}$$

$$\omega b = ks\,\omega[[(v_f/v_c)\cos\varphi - 1]. \tag{A2}$$

Here k_s denotes the spring constant of the force-measuring spring in the apparatus and ϕ denotes phase of the output voltage relative to input.

Omitting the elastic terms, the viscous contribution in Eq. (A2) can be quantified as the effective viscosity,

$$\eta_{\text{eff}} = \omega b D/A, \tag{A3}$$

where the symbols have the same meaning as in the above equations. This model also allows us to accurately account for device compliance, since this also contributes to shear forces.[33]

The sensitivity is limited by the absolute phase change that can be detected. Using lock-in amplifiers the resolution is typically 0.1° with oscillation amplitude of a few tenths of a nanometer. Better resolution is possible when the amplitude is larger.

Consider the viscosity that can be measured by these two methods, steady shear and dynamic shear. For forces measuring by spring displacement in steady shear, the resolution of $\pm 0.5\ \mu$N has been reported.[12] Thus for a shear rate of[8] 20 nm s^{-1} the minimum viscosity detectable is $\approx 10^3$ Pa s, which is already 6 orders of magnitude higher than that of bulk OMCTS. In the case of forces measured by dynamic oscillatory motion (this paper), a minimum change of phase by 0.1° corresponds to a viscosity of 0.5 Pa s when using a drive at 100 Hz.

2. Issue of linearity of nonlinearity of response

Rheologists familiar with viscoelastic materials are well aware that viscosity depends on shear rate. Deformations on the order of nanometers may seem negligible but, in considering the effective shear rate, the relevant quantity is the velocity normalized by film thickness. The effective viscosity is known to decrease markedly when a critical (low) level of shear rate is exceeded.[9] Whenever the shear rate is so large as to give a nonlinear response, the effective viscosity of the unperturbed film is surely underestimated. Much of the nanorheology data in the surface forces and AFM literature refers to nonlinear responses.

3. The issue of experimental geometry

The surface forces apparatus confines liquids between two crossed cylinders; the geometry is approximated as a sphere against a flat plate. The measured quantity is the force required to translate this sphere parallel to the flat plate. For this case the continuum hydrodynamics was worked out long ago and is given by

$$F_F = (16\pi/5)(vR\eta)\ln(R/b_0), \tag{A4}$$

where v is the shear velocity, R is the sphere radius, η is the viscosity, and b_0 is the closest separation between the sphere and the plate.[47] Clearly, with a curved geometry, any shear measurement probes the state of the liquid over a range of film thickness. The contribution to the total force from the point of closest approach dominates only if the viscosity in this region exceeds that farther away.

When a sphere is flattened at the apex, as under a Hertzian contact, this is approximated as a parallel-plate shear geometry and the shear force can be written,

$$F_s = \eta v A/D, \tag{A5}$$

where A denotes area, D denotes film thickness, and the other symbols have the same meaning as in Eq. (A1). This is appropriate to use provided that the viscosity of the confined liquid is enhanced by at least 1–2 orders of magnitude over that of the liquid outside the zone of closest approach.

When dealing with Eqs. (A4) and (A5), the effective contact areas, from which viscosity is calculated, are obviously very different. The resulting danger of comparing experiments performed with curved and flattened surface geometry is evident. If one compares Eqs. (A4) and (A5) for a

Downloaded 25 Jul 2001 to 130.126.103.150. Redistribution subject to AIP license or copyright, see http://ojps.aip.org/jcpo/jcpcr.jsp

lateral radius of only 7 μm away from the centerpoint of closest approach (the lateral distance over which the thickness of the confined film changes by typically 2–4 molecular diameters), one obtains $F_S/F_F=24$. Therefore, simply the choice of Eq. (A4) or (A5) results in more than 1 order of magnitude different of imputed viscosity from the same force measurement.

4. Resolution in determining a first-order transition of shear response

Now having a fair understanding of the differences between the dynamic surface forces instruments used in various laboratories, let us consider the arguments for a first-order phase transition in confined fluids. Recent studies reported a transition to solidity, with diminishing film thickness, so abrupt as to seem first-order when the film thickness passed from 7 to 6 molecular dimensions.[13,14]

Reflection shows that the claim of an abrupt transition is actually consistent with the opposite interpretation. First, in those experiments,[13,14] elastic and viscous forces were not discriminated. Secondly, the uncertainty of ± 0.5 μN potentially amounted to a considerable effective viscosity—estimated above to amount to perhaps 6 orders of magnitude larger than that of the bulk liquid. Third, the difference between the effective viscosity calculated from Eqs. (A4) and (A5) was not distinguished.

[1] J. Van Alsten and S. Granick, Phys. Rev. Lett. **61**, 2570 (1988).
[2] J. N. Israelachvili and P. M. McGuiggan, Science **241**, 795 (1988).
[3] S. Granick, A. L. Demirel, L. Cai, and J. Peanasky, Isr. J. Chem. **35**, 75 (1995).
[4] R. Zallen, *The Physics of Amorphous Solids* (Wiley, New York, 1998).
[5] R. Defay, L. Prigogine, A. Bellemans, and D. H. Everett, *Surface Tension and Adsorption* (Longman, London, 1996).
[6] C. L. Jackson and G. B. McKenna, Chem. Mater. **8**, 2128 (1996).
[7] K. Katsumi, A. Watanabe, T. Iiyama, R. Rhadakrishnan, and K. E. Gubbins, J. Phys. Chem. B **103**, 7062 (1999).
[8] S. Kawana and R. A. L. Jones, Phys. Rev. E **63**, 021501 (2001).
[9] S. Granick, Science **253**, 1374 (1991).
[10] S. Granick, Phys. Today **52**, 26 (1999).
[11] B. Bhushan, J. N. Israelachvili, and U. Landman, Nature (London) **374**, 607 (1995).
[12] J. Klein, J. Phys.: Condens. Matter **12**, A19 (2000).
[13] E. Kumacheva and J. Klein, Science **269**, 5225 (1995).
[14] E. Kumacheva and J. Klein, J. Chem. Phys. **108**, 7010 (1998).
[15] A. L. Demirel and S. Granick, Phys. Rev. Lett. **77**, 2261 (1996).
[16] S. Nasuno, A. Kudrolli, A. Bak, and J. P. Gollub, Phys. Rev. E **58**, 2161 (1998).
[17] S. A. Langeer and A. J. Liu, Europhys. Lett. **49**, 68 (2000).
[18] M. Schoen, C. L. Rhykerd, D. J. Diestler, and J. H. Cushman, Science **245**, 1223 (1989).
[19] P. A. Thompson and M. O. Robbins, Science **250**, 792 (1990).
[20] J. P. Gao, W. P. Luedtke, and U. Landman, Phys. Rev. Lett. **79**, 705 (1997).
[21] J. E. Curry, J. Chem. Phys. **113**, 2400 (2000).
[22] P. A. Thompson, G. S. Grest, and M. O. Robbins, Phys. Rev. Lett. **68**, 3448 (1992).
[23] K. S. Schweizer (private communication).
[24] R. Khare, J. de Pablo, and A. Yethiraj, J. Chem. Phys. **114**, 7593 (2001).
[25] J. N. Israelachvili and G. E. Adams, J. Chem. Soc., Faraday Trans. **74**, 975 (1978).
[26] R. G. Horn and J. N. Israelachvili, Chem. Phys. Lett. **71**, 192 (1980).
[27] R. G. Horn and J. Israelachvili, J. Chem. Phys. **75**, 1400 (1981).
[28] H. K. Christenson, D. W. R. Gruen, R. G. Horn, and J. N. Israelachvili, J. Chem. Phys. **87**, 1834 (1987).
[29] J. P. Gao, W. P. Luedtke, and U. Landman, J. Phys. Chem. B **101**, 4013 (1997).
[30] S. J. O'Shea, M. E. Welland, and J. B. Pethica, Chem. Phys. Lett. **223**, 336 (1994).
[31] J. D. Ferry, *Viscoelastic Properties of Polymers*, 3rd ed. (Wiley, New York, 1980).
[32] H.-W. Hu and S. Granick, Science **258**, 1339 (1992).
[33] S. Granick and H.-W. Hu, Langmuir **10**, 3857 (1994).
[34] A. L. Demirel and S. Granick, J. Chem. Phys. **109**, 6889 (1998).
[35] J. Peachey, J. Van Alsten, and S. Granick, Rev. Sci. Instrum. **62**, 463 (1991).
[36] Y. Zhu and S. Granick, J. Rheol. **44**, 1169 (2000).
[37] J. Peanasky, H. M. Schneider, C. R. Kessel, and S. Granick, Langmuir **11**, 953 (1995).
[38] G. Reiter, A. L. Demirel, and S. Granick, Science **263**, 1741 (1994).
[39] A. Levent Demirel and S. Granick, Phys. Rev. Lett. **77**, 4330 (1996).
[40] L. Cai and S. Granick, in *Micro/Nanotribology and its Applications*, NATO ASI Series, edited by B. Bhushan (Kluwer Academic, Boston, 1997).
[41] N. W. Tschoegl, *The Phenomenological Theory of Linear Viscoelastic Behavior* (Springer-Verlag, New York, 1989).
[42] W. Götze and L. Sjögren, Rep. Prog. Phys. **55**, 241 (1992).
[43] T. G. Mason and D. A. Weitz, Phys. Rev. Lett. **75**, 2770 (1995).
[44] H. Z. Cummins, G. Li, W. M. Du, and J. Hernandez, Physica A **204**, 169 (1994).
[45] P. J. Davis and D. J. Evans, J. Chem. Phys. **100**, 541 (1994).
[46] A. Dhinojwala, L. Cai, and S. Granick, in *Dynamics in Small Confining Systems*, edited by J. M. Drake, J. Klafter, and R. Kopelman (Materials Research Society, New York, 1997).
[47] J. Happel and H. Brenner, *Low Reynolds Number Hydrodynamics* (Kluwer, The Netherlands, 1983).

Downloaded 25 Jul 2001 to 130.126.103.150. Redistribution subject to AIP license or copyright, see http://ojps.aip.org/jcpo/jcpcr.jsp